

## Design of Radiating *K*-Band HEMT Oscillators by Means of Moment-Method Approach

Martin M. Kaleja and Erwin M. Biebl

**Abstract**—This paper discusses the design of radiating *K*-band oscillators with high electron-mobility transistors (HEMT's) as active devices. In order to allow monolithic integration, the design is based on a uniplanar microstrip configuration, i.e., all terminals of the passive microstrip circuit are located on top of the substrate and no via-holes are needed. In this configuration, feeding of the microstrip lines is incompatible to the fundamental quasi-TEM microstrip mode. Moreover, the radiation losses of these so-called active antennas significantly influence the oscillation condition. Thus, modeling of the passive circuit by means of a full-wave analysis is mandatory. In this paper, we show how a full-wave analysis of the passive circuit can be combined with well-known network-based oscillator design methods using commercially available design tools. By using a moment-method approach for the passive structure and small-signal model for the active device, all relevant electromagnetic effects, like losses, coupling and radiation, are included, allowing a very precise prediction of the operation frequency.

**Index Terms**—Active integrated circuit, HEMT, oscillator.

### I. INTRODUCTION

Integration of an active device with a resonant, radiating, and passive structure in the proper way results in a radiating oscillator, which is commonly called an active (integrated) antenna [1]. This concept exhibits many advantages, e.g., minimizing the losses and increasing the effective length and bandwidth of the radiating patch, and provides a small inexpensive quasi-optical frontend for future high-volume millimetric applications, e.g., wireless communication, automotive sensor systems, and wireless local area networks [2].

The basic idea behind radiating oscillators, namely the spatial coincidence of several functions like signal generation and radiation, complicates the design. Since significant radiation is desired, classical quasi-static approaches are no longer sufficient. Although sophisticated full-wave analysis methods are available in commercial microwave design software, a combination with oscillator design tools usually based on network models is not possible. Moreover, for low-cost applications, via-holes have to be avoided. Thus, only uniplanar microstrip configurations, where terminals of the passive microstrip circuit are located on top of the substrate, are acceptable. In this configuration, feeding of the microstrip lines is incompatible to the fundamental quasi-TEM microstrip mode. In this paper, we demonstrate the design of active antennas by means of commercially available software, implementing well-known oscillator theories and both quasi-static and moment-method-approach algorithms.

Radiating oscillators can be realized using either two- or three-terminal elements as active devices. Two-terminal devices, like IMPATT diodes, have been used for some time in active antennas [3] and heterojunction bipolar transistors (HBT's) as three-terminal devices were recently reported [4]. This paper investigates for the first time the use of high electron-mobility transistors (HEMT's) in active *K*-band antennas. The additional degree of freedom using a transistor is applied to consider the behavior of all transistor terminals,

Manuscript received November 12, 1997; revised May 12, 1998.

The authors are with Fachgebiet Optische und Quasi-Optische Systems, Lehrstuhl fuer Hochfrequenztechnik, Technische Universitaet Muenchen, 80333 Munich, Germany.

Publisher Item Identifier S 0018-9480(98)06732-5.

in particular, the source terminal to satisfy oscillation condition. In addition to earlier published works [5], we fit measured two-port *S*-parameters into full-wave analysis. The connection between the transistor and the microstrip structure is realized in flip-chip technology that can be simulated using suitable models.

Starting from the modeling of the transistor and of the passive microstrip structure, this paper goes through the design of the oscillators applying both two- and three-port oscillator theories. After simulation, two different concepts are realized. Fabrication of the oscillators is done by means of flip-chip-bonding of the HEMT's. Finally, the realized antennas are measured and the results are compared with calculated data.

### II. MODELING

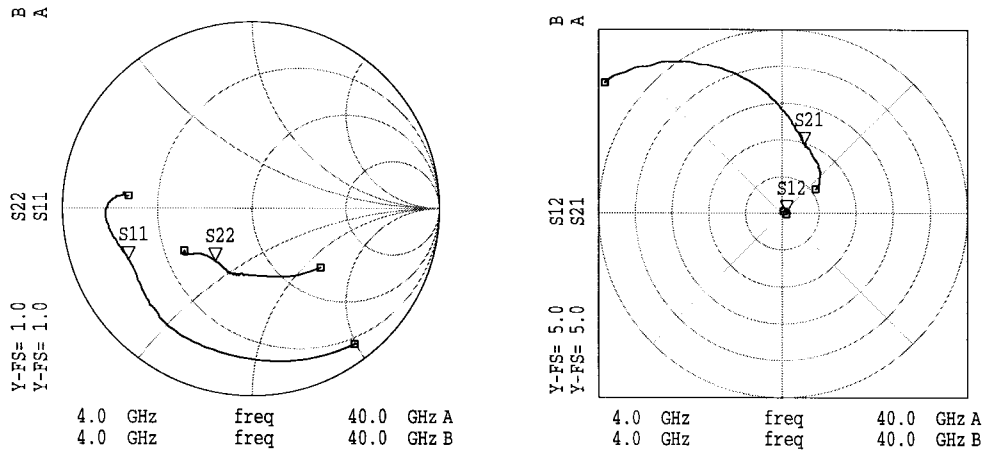
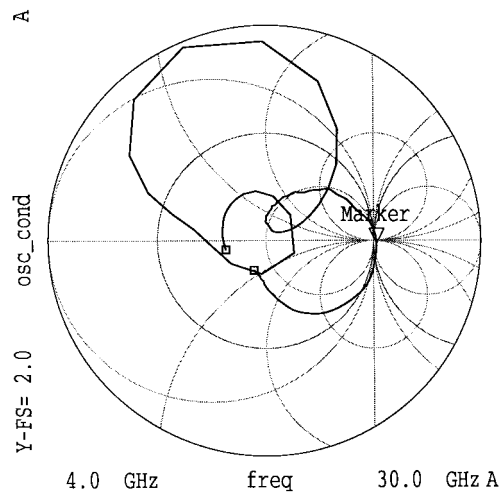
#### A. HEMT Device Model

Precise modeling of oscillators usually requires a large-signal analysis, where the behavior of the passive part must be known not only at the fundamental frequency, but also at the first few harmonics [6]. Employing full-wave analysis of the passive circuit in combination with a large-signal analysis results in very high numerical effort, since for higher harmonics, the discretization grid applied to the passive circuit has to be refined proportionally to the frequency. Thus, we use a small-signal model for oscillator design. We will show that the small-signal model predicts the oscillation frequency with sufficient accuracy.

Our small-signal model is based on measurements of the scattering parameters in a common-source configuration. For measurement, we bonded the transistor t409d, manufactured by Siemens, Germany, on a coplanar test structure. According to the manufacturer's recommendations,  $U_{ds} = 2.5$  V and  $I_d = 26$  mA were applied. We measured the two-port scattering parameters using an HP 8510 network analyzer and a Cascade wafer prober and imported the data in an HP MDS for simulation. Fig. 1 gives the scattering parameters ( $Z_0 = 50 \Omega$ ) in a common-source configuration. The readings of the markers at 24 GHz are  $|S_{11}| = 0.71$ ,  $\angle S_{11} = -157^\circ$ ,  $|S_{12}| = 0.12$ ,  $\angle S_{12} = 2^\circ$ ,  $|S_{21}| = 1.95$ ,  $\angle S_{21} = 72^\circ$ ,  $|S_{22}| = 0.34$ ,  $\angle S_{22} = -124^\circ$ .

#### B. Passive Structure Model

Application of commercial design tools based on full-wave methods like HP Momentum is restricted to a few standardized feeding configurations provided by the software. In general, uniplanar feeding of microstrip lines is not included. Our integral-equation solver [7] based on the method of moments considers the fact that the feeding of the passive structure is incompatible with the fundamental quasi-TEM mode of microstrip lines. We developed a set of test structures and analyzed them using our own and commercially available software tools. We found that the HP MDS and HP Momentum analysis procedures can be used for uniplanar microstrip structures if we used the “point-feed” port and small line width  $w < 0.05\lambda_0$ . The quasi-static approach MDS allows the optimization of the circuit's *S*-parameters, but considers the effects of coupling and resistive losses as well as leakage phenomena only with standardized models. These effects are taken into consideration by the moment-method approach (Momentum). However, optimization is not possible with the latter model. We combined these two approaches recursively for our designs.

Fig. 1. Measured  $S$ -parameter of the t409d transistor.Fig. 2.  $\Gamma_{IN} \cdot \Gamma_L$  shown in Smith-Chart representation.

### III. OSCILLATOR DESIGN

Traditional oscillator theories can be divided into two- and three-port theories. We applied both to compare their results and to prove their feasibility using model-design software.

#### A. Two-Port Oscillator Design

In this design, both the transistor and embedding circuit are considered as two-ports to satisfy the oscillation condition. In compliance with the theory described in [8], the patches at both ports of the transistor are designed independently of each other. Firstly, the dimensions of the patch at the gate terminal were determined using stability circles to satisfy  $|\Gamma_{IN}| > 1$ , where  $\Gamma_{IN}$  represents the reflection coefficient of the transistor's drain port with the gate connected to the gate patch. Secondly, the patch at the drain terminal  $\Gamma_L$  was designed to satisfy the oscillation conditions  $|\Gamma_{IN}| \cdot |\Gamma_L| \geq 1$  and  $\angle \Gamma_{IN} + \angle \Gamma_L = 2\pi n$  ( $n = 0, 1, 2, \dots$ ), respectively. Fig. 2 shows the product  $\Gamma_{IN} \cdot \Gamma_L$  in Smith-Chart representation. The reading of the marker set at 22.5 GHz is  $\Gamma_{IN} \cdot \Gamma_L = 1.054$ .

Each circuit was first designed using a quasi-static approach, and then to include radiation effects, using the method-of-moments approach. Due to the current distribution derived from the full-wave simulation, the bias networks, each consisting of a radial-stub bias circuit, were connected to the microstrip patches at the position of maximum current density. In Fig. 3, the quarter-wave open-circuit

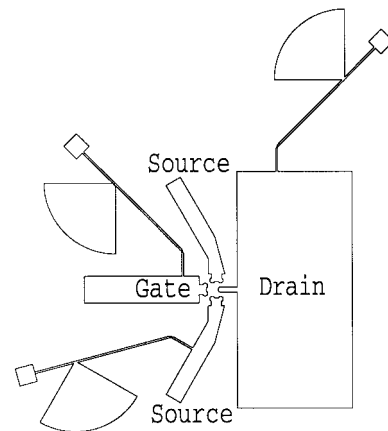


Fig. 3. Realized design using two-port oscillator theory.

lines at the source terminal (length: 831  $\mu\text{m}$ , width: 187  $\mu\text{m}$ , distance between bias network and open end: 641  $\mu\text{m}$ ) are bent to minimize coupling effects. The gate line is a quarter-wave resonator (length: 1289  $\mu\text{m}$ , width: 300  $\mu\text{m}$ , distance between bias network and open end: 1109  $\mu\text{m}$ ) and the drain patch (length: 1310  $\mu\text{m}$ , width: 2677  $\mu\text{m}$ , distance between bias network and open end: 861  $\mu\text{m}$ ) represents the load for the transistor.

#### B. Three-Port Oscillator Design

Alternatively, the transistor is considered as a three-port device [9]. Application of three-port theory [10] requires a three-port scattering-matrix representation of the HEMT. Transformation of the measured two-port common-source representation into a three-port representation has been reported in [11].

The active and passive portion of the active antenna are simulated as three-ports to consider all coupling effects of the structure and to allow for parallel feedback loops. In a first step, some of the coupling effects are considered by approximation using the quasi-static coupled transmission-line model included in MDS to estimate the oscillator's behavior. In a second step, all of the coupling effects are considered by means of full-wave analysis that also gives information about correct placement of the bias networks. The oscillation condition  $|\det(\mathbf{S} \cdot \mathbf{S}' - \mathbf{E})| \geq 0$  and  $\text{Arg} \{ \det(\mathbf{S} \cdot \mathbf{S}' - \mathbf{E}) \} = 0$  is visualized in Fig. 4 using the moment-method approach for the passive structure. According to [9],  $\mathbf{S}$  and  $\mathbf{S}'$  represent the transformed three-port scattering matrix of the HEMT and the three-port scattering matrix of

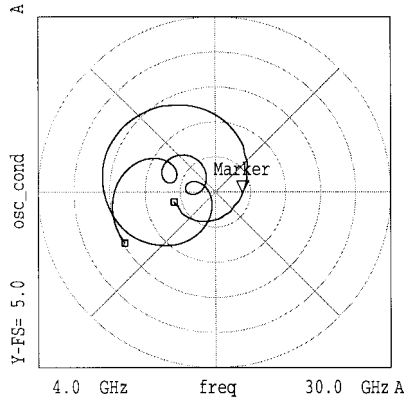
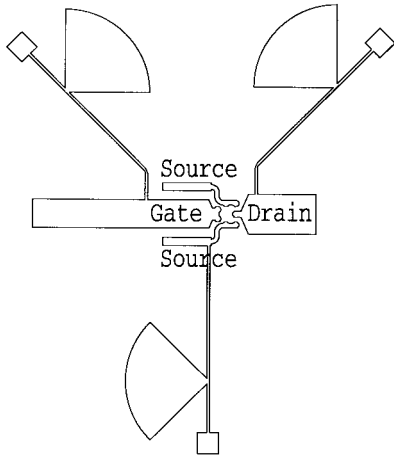
Fig. 4. Visualization of  $\det(\mathbf{S} \cdot \mathbf{S}' - \mathbf{E})$  using moment-method approach.

Fig. 5. Realized design using three-port oscillator theory.

the passive circuit, respectively.  $\mathbf{E}$  is the identity matrix. The reading of the marker set at 24 GHz is  $\det(\mathbf{S} \cdot \mathbf{S}' - \mathbf{E}) = 0.773$ .

The layout is shown in Fig. 5. Coupling between the source line (length: 458  $\mu\text{m}$ , width: 74  $\mu\text{m}$ , distance between bias network and open end: 428  $\mu\text{m}$ ) and the half-wave gate resonator (length: 1698  $\mu\text{m}$ , width: 274  $\mu\text{m}$ , distance between bias network and open end: 1046  $\mu\text{m}$ ) realizes a parallel feedback loop. The distance between both lines is 94  $\mu\text{m}$ . The load for the transistor is again the drain patch (length: 721  $\mu\text{m}$ , width: 387  $\mu\text{m}$ , distance between bias network and open circuit: 556  $\mu\text{m}$ ).

### C. Comparison of the Two Designs

In order to check the two designs derived from different theories, both designs are finally calculated using three-port theory and the moment-method approach. We found that two-port design is not sufficient for modeling an active antenna in the *K*-band since some coupling effects causing spurious oscillators could not be taken into account.

## IV. REALIZATION

The oscillators are realized on  $\text{Al}_2\text{O}_3$  ceramic substrates with a relative dielectric constant of 9.9, thickness of 10 mil, and gold metallization of 2 mil. The AlGaAs/InGaAs-chip HEMT's ( $280 * 330 \mu\text{m}^2$ ) are mounted on the substrate using flip-chip technology. The pads of the transistor ( $\varnothing 65 \mu\text{m}$ ) are contacted to gold bumps placed on the terminals of the passive circuit using the thermo-

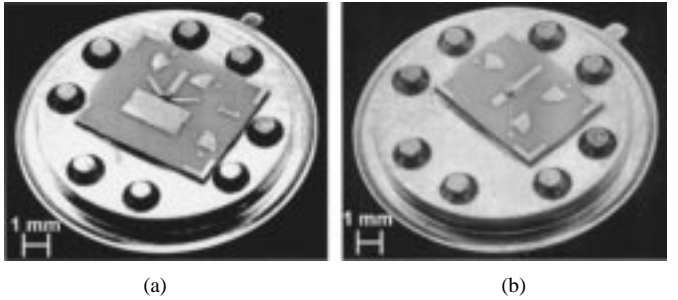


Fig. 6. Photographs of the realized active antennas using (a) two-port and (b) three-port oscillator theory.

TABLE I  
MODELED AND MEASURED FREQUENCIES OF THE REALIZED DESIGNS

Design	f predicted [GHz]	f measured [GHz]	measured output power
Two-port	22.55	22.48 - 22.60	9.1 - 10 dBm
Three-port	24.00	23.96 - 24.06	8.8 - 9.2 dBm

compression technique. The substrates are glued on TO8 headers with nail-head pins that are compatible with the 0.1-in grid (see Fig. 6).

## V. MEASUREMENTS

Multiple samples of the realized designs are measured using an HP 70 000 modular spectrum analyzer to certify the theories presented above. Bias was chosen in accordance with the simulation:  $U_{ds} = 2.5 \pm 0.2$  V and  $I_d = 26 \pm 3$  mA. It could be shown that the results of the full-wave analysis are in accordance with the actual behavior of the active antennas. Table I shows the predicted and measured frequencies of operation. Both designs exhibit excellent reproducibility. The span of operation frequencies given in Table I was measured with more than ten different oscillators for both designs.

The difference between the simulated and measured operation frequency is smaller than 70 MHz. That is equivalent to 0.3%. Both designs show a high radiated output power of almost 10 mW.

## VI. CONCLUSION

Well-known network-based small-signal oscillator theories have been combined with microwave-design software based on full-wave analysis. Both two- and three-port design procedures have been investigated. It has been found that due to significant coupling effects within the passive structure, only three-port design procedures provide acceptable accuracy.

Two different designs of radiating oscillators were realized by means of flip-chip technology. The deviations between the predicted and measured operation frequency are (even though a small-signal model is used) less than 0.3%.

The method presented in this paper allows the reliable design of (monolithic) integrated radiating oscillators based on uniplanar microstrip circuits. These active antennas for the lower millimeter-wave range are key components for future low-cost radar and communication systems.

## ACKNOWLEDGMENT

The HEMT's were provided by and bonded at Siemens-ZT, Munich, Germany. The contributions of P. Heide and T. von Kerssenbrock are acknowledged by the authors.

## REFERENCES

- [1] J. Lin and T. Itoh, "Active integrated antennas," *IEEE Trans. Microwave Theory Tech.*, vol. 42, pp. 2186-2193, Dec. 1994.
- [2] T. Itoh, "Quasioptical microwave circuits for wireless applications," *Microwave J.*, vol. 38, no. 1, pp. 64-85, Jan. 1995.
- [3] J.-F. Luy and P. Russer, *Silicon-Based Millimeter-Wave Devices*. Berlin, Germany: Springer-Verlag, 1994.
- [4] M. J. Kelly, J. A. C. Stewart, and A. D. Patterson, "HBT active antenna as a self-oscillating Doppler sensor," in *IEEE MTT-S Int. Microwave Symp. Dig.*, Denver, CO, June 18-13, 1997, pp. 1065-1068.
- [5] J. Birkeland and T. Itoh, "Planar FET oscillators using periodic microstrip patch antennas," *IEEE Trans. Microwave Theory Tech.*, vol. 37, pp. 1232-1236, Aug. 1989.
- [6] M. Schwab, "Determination of the steady state of an oscillator by a combined time-frequency method," *IEEE Trans. Microwave Theory Tech.*, vol. 39, pp. 1391-1402, Aug. 1991.
- [7] M. O. Thieme and E. M. Biebl, "A fast and rigorous synthesis procedure for (monolithic) millimeter-wave integrated circuit layout," in *IEEE MTT-S Int. Microwave Symp. Dig.*, Denver, CO, June 8-13, 1997, pp. 1009-1012.
- [8] G. Gonzalez, *Microwave Transistor Amplifiers*. Englewood Cliffs, NJ: Prentice-Hall, 1984.
- [9] A. S. Khanna, "Parallel feedback FETDRO design using 3-port *S*-parameters," in *IEEE MTT-S Int. Microwave Symp. Dig.*, San Francisco, CA, June 1984, pp. 181-183.
- [10] I. J. Bahl and P. Bhartia, *Microwave Solid State Circuit Design*. New York: Wiley, 1988.
- [11] A. S. Khanna, "Three-port *S*-parameters ease GaAs FET designing," *Microwave RF*, vol. 24, no. 12, pp. 81-84, Nov. 1985.

## Nonlinear Modeling and Design of Bipolar Transistors Ultra-Low Phase-Noise Dielectric-Resonator Oscillators

M. Regis, O. Llopis, and J. Graffeuil

**Abstract**—This paper presents a design methodology for low phase-noise dielectric-resonator oscillators (DRO's) with applications examples at 4 GHz. Different oscillators topologies are investigated and, finally, three oscillators' configurations have been simulated, realized in discrete elements, and characterized. The best measured phase-noise magnitude is  $-133$  dBc/Hz at 10-kHz offset frequency.

### I. INTRODUCTION

Precise frequency generation is an essential function in telecommunications or radars applications. The phase-noise modeling in microwave free-running oscillators has been a subject of research for many years, but many problems remain unsolved and make the nonlinear design approach very difficult [1]-[5]. However, because of the availability of efficient commercial nonlinear software, it would be appropriate to base the design of low phase-noise dielectric-resonator oscillators (DRO's) only on the classical small-signal approach [6].

The aim of this paper is to demonstrate that the nonlinear simulation, in spite of being able to predict in all cases the exact phase-noise level of the oscillator, is still a good tool to check if a circuit topology

Manuscript received November 3, 1997; revised April 14, 1998.

M. Regis and J. Graffeuil are with LAAS-CNRS, 31077 Toulouse Cedex 04, France, and also with Université Paul Sabatier, 31062 Toulouse Cedex, France.

O. Llopis is with LAAS-CNRS, 31077 Toulouse Cedex, France.

Publisher Item Identifier S 0018-9480(98)06733-7.

is appropriate for a low phase-noise design. As an example, problems of impedance matching and resonator decoupling are discussed for parallel-feedback oscillators and compared to empirical rules often used by engineers in that field.

Since in this paper our main interest is on ultra-low phase-noise DRO's, only silicon bipolar junction transistors (BJT's) oscillators are investigated. The selected devices feature very good performances in terms of low-frequency (LF) noise, which are still unreached by heterojunction bipolar transistors (HBT's) technology. We found that only some carefully selected devices in the Si/SiGe HBT family could reach these noise levels, with the advantage of higher gain and cutoff frequency compared to the BJT. This study is actually a preliminary study for the design of ultra-low phase-noise Si/SiGe HBT oscillators, but the first results obtained with these devices will be published elsewhere [7]. In this paper, we will focus on oscillator design and topology.

The paper is organized as follows. Section II describes the circuit elements and operating conditions. In Section III, we propose a phase-noise-simulation approach based on input LF, the phase-noise measurements' results obtained on the different oscillators. Finally, these results are compared to the simulation results of Section IV.

### II. CIRCUITS ELEMENTS AND OPERATING CONDITIONS

Various high-frequency BJT devices are commercially available, but they all feature different LF noise characteristics. A preliminary test is necessary before choosing a device for a low phase-noise-oscillator application. This can be done either by measuring the LF noise on the quiescent (or nonoscillating) device or by measuring the amplifier-device residual phase noise or directly by measuring the phase noise of test oscillators in which the device is embedded [8]. None of these methods is totally rigorous, but the three give valuable information and almost always converge to the same device classification. The Hewlett-Packard Si-BJT AT41400 has thus been selected. It features an extremely low input voltage noise level of about  $0.4$  nV/ $\sqrt{\text{Hz}}$  at 1 kHz (see Fig. 1, curve 2) compared with other devices of the same type [9] and is easily able to sustain a 4-GHz oscillation. The bias conditions are approximately  $I_c = 30$  mA and  $V_{ce} = 4$  V (see Section III).

The passive part of the oscillator is realized with a Murata's U dielectric resonator featuring an unloaded *Q*-factor ( $Q_o$ ) of 8000. This dielectric resonator is supported by a Teflon rod and used in transmission or in reflection modes. In the transmission configuration, it is placed in a metallic housing (copper) and the coupling adjustment is done by magnetic probes. In the reflection configuration, the dielectric resonator is placed near a  $50\Omega$  microstrip line on an alumina substrate.

### III. PHASE-NOISE-SIMULATION METHOD

In microwave oscillators, the phase noise is generally attributed to the active device LF noise. This LF noise is converted into frequency fluctuations by a nonlinear mixing process. The classical modeling method uses two noise sources (current and voltage) referred to the transistor input [2], [9]-[12]. The LF noise is measured on the nonoscillating device, and the phase-noise calculation is performed either by using a conversion matrix method, which consists of studying a low-level phase-modulation processor or by using a pushing-factor approach.

The pushing-factor approach is based on the assumption that the device LF equivalent circuit is almost constant in the LF noise